Heliyon 10 (2024) e24012

Contents lists available at ScienceDirect

Heliyon

journal homepage: www.cell.com/heliyon

Nitidine chloride inhibits G2/M phase by regulating the p53/14-3-3 Sigma/CDK1 axis for hepatocellular carcinoma treatment

Bo Zhang [a,1], Bo Zhou [a,1], Guihong Huang [d,e,f,1], Jing'an Huang [a], Xiaoxin Lin [a], Zonghuai Li [a], Yuanchu Lian [a], Qiujie Huang [g,**], Yong Ye [b,c,*]

[a] *Scientific Research Center, Guilin Medical University, Guilin, China*
[b] *School of Pharmacy, Guangxi Medical University, Guangxi, China*
[c] *Guangxi Key Laboratory of Bioactive Molecules Research and Evaluation, China*
[d] *Department of Pharmacy, The Second Affiliated Hospital of Guilin Medical University, Guilin, China*
[e] *Guangxi Health Commission Key Laboratory of Glucose and Lipid Metabolism Disorders, Key Laboratory of Diabetic Systems Medicine, The Second Affiliated Hospital of Guilin Medical University, Guilin, Guangxi, 541199, China*
[f] *Guangxi Key Laboratory of Drug Discovery and Optimization, Guangxi Engineering Research Center for Pharmaceutical Molecular Screening and Druggability Evaluation, School of Pharmacy, Guilin Medical University, Guilin, Guangxi, 541199, China*
[g] *Guangxi University of Chinese Medicine, Teaching Experiment and Training Center, Nanning, China*

ARTICLE INFO

Keywords:
Nitidine chloride
Hepatocellular carcinoma
Network pharmacology
Cell cycle
p53/14-3-3 Sigma/CDK1 axis

ABSTRACT

Background: Liver cancer had become the sixth most common cancer. Nitidine chloride (NC) has demonstrated promising anti-HCC properties; however, further elucidation of its mechanism of action is necessary.
Methods: The anti-HCC targets of NC were identified through the utilization of multiple databases and ChIPs data analysis. The GO and KEGG analyses to determine the specific pathway affected by NC. The Huh 7 and Hep G2 cells were subjected to a 24-h treatment with NC, followed by evaluating the impact of NC on cell proliferation and cell cycle. The involvement of the p53/14-3-3 Sigma/CDK1 axis in HCC cells was confirmed by qPCR and WB analysis of the corresponding genes and proteins.
Results: The GO and KEGG analysis showed the targets were related to cell cycle and p53 signaling pathways. In vitro experiments showed that NC significantly inhibited the proliferation of HCC cells and induced G2/M phase arrest. In addition, qPCR and WB experiments showed that the expression of p53 in HCC cells increased after NC intervention, while the expression of 14-3-3 Sigma and CDK1 decreased.
Conclusion: NC can inhibit the proliferation of HCC cells and induce G2/M cell cycle arrest, potentially by regulating the p53/14-3-3 Sigma/CDK1 axis.

1. Introduction

Worldwide, an estimated 19.3 million new cancer cases and almost 10.0 million cancer deaths occurred in 2020. Among them, liver

* Corresponding author. School of Pharmacy, Guangxi Medical University, Guangxi, China.
** Corresponding author.
E-mail addresses: hqj8@163.com (Q. Huang), yong-ye@163.com (Y. Ye).
[1] These authors have contributed equally to this work.

https://doi.org/10.1016/j.heliyon.2024.e24012
Received 22 October 2023; Received in revised form 29 December 2023; Accepted 2 January 2024
Available online 3 January 2024

cancer (4.7 %) had become the sixth most common cancer after female breast cancer (11.7 %), lung (11.4 %), colorectal (10.0 %), prostate, (7.3 %) and stomach (5.6 %) cancers. At the same time, liver cancer (8.3 %) was also the third leading cause of death after lung (18 %) and colorectal (9.4 %) cancers. It is worth mentioning that hepatocellular carcinoma (HCC) accounted for 75%–85 % of liver cancer cases [1]. These data indicate that liver cancer had a significant negative impact on the health and lives of people.

As was well known, the onset of liver cancer is often not caused by a single factor. The common inducing factors of liver cancer mainly include virus infection, exposure to toxic chemicals, liver injury, etc [2]. A study demonstrated an exceedingly strong association between infection with Hepatitis B virus (HBV) or Hepatitis C virus (HCV) and the development of liver cancer [3]. Chronic HBV infection is involved in the progression of HCC through various mechanisms, including integration of HBV DNA, induction of cellular stress response, deactivation of HCC pathways, and support of HDV replication [4]. HCV is able to induce oxidative stress damage in the liver, resulting in hepatic inflammation and cell apoptosis, ultimately progressing to liver cancer [5]. Aflatoxin is one of the most potent natural carcinogens discovered to date [6]. Epidemiological studies consistently demonstrate a significant increase in the risk of HCC associated with exposure to aflatoxin, which could even act synergistically with chronic HBV infection to augment the risk [7]. In addition, end-stage liver damage caused by alcohol-related fatty liver disease or non-alcoholic steatohepatitis (NASH) induce by overnutrition could also trigger the development of liver cancer [8]. Unfortunately, despite a relatively thorough understanding of the occurrence of liver cancer, its treatment methods remained unsatisfactory. Currently, in clinical practice, the main treatment options for liver cancer include surgical resection, as well as radiation and chemotherapy [9]. However, drug resistance often posed a daunting challenge to chemotherapy in the treatment of liver cancer patients. Consequently, the search for novel and potent anti-cancer agents for liver cancer had become an urgent research priority. Interestingly, numerous studies increasingly demonstrate that the progression of liver cancer can be effectively impeded by arresting the cell cycle of liver cancer cells [10–12]. Consequently, the quest for compounds capable of arresting the cell cycle in liver cancer and uncovering their mechanisms of action holds paramount importance in advancing the development of novel anti-liver cancer medications.

Zanthoxylum nitidum (Roxb.) DC., which was included in quality standard of Zhuang medicinal material in Guangxi Zhuang Autonomous Region (Volume I), was used to treat neuralgia, toothache, rheumatism, traumatic injury, venomous snake bites and various types of cancer [13,14]. Numerous studies have demonstrated that various chemical constituents of *Zanthoxylum nitidum* (Roxb.) DC exhibit significant inhibitory activity against different types of cancer [15,16]. Nitidine chloride (NC) was one of the primary active components of *Zanthoxylum nitidum* and possessed a broad spectrum of anti-cancer activity. Studies demonstrated that NC inhibited various types of cancer cells, including ovarian cancer, breast cancer, gastric cancer, liver cancer, glioblastoma, and osteosarcoma, among others. The mechanism underlying NC's anti-cancer activity may have involved inducing apoptosis of tumor cells, inhibiting tumor cell migration and invasion, and regulating multiple signaling pathways [17–21]. In the treatment of HCC, NC was reported to inhibit the growth and induce apoptosis of HCC cells by regulating multiple signaling pathways such as JAK1/STAT3, JNK/c-Jun, ERK, and SHH [22–24]. Moreover, NC could induce HCC cells apoptosis by upregulating p53, p21, and Bax and downregulating Bcl-2 [25]. However, in order to facilitate the clinical application of NC, further research is needed to investigate its mechanisms of action in HCC.

In this study, we will utilize network pharmacology to further investigate the mechanism of NC's anti-HCC effects. To ensure the specificity of HCC targets, we employed a rigorous methodology. Initially, we meticulously selected the chip that had been confirmed as HCC in the GEO database. Subsequently, we utilized the differential genes present within the chip, which distinguished between normal and tumor tissues, as our HCC targets for further research. Our research aims to deepen our understanding of the mechanism of action of NC in the treatment of HCC. By doing so, we aim to establish a solid foundation for the clinical development of NC.

2. Methods

2.1. Acquisition of NC targets

After obtaining the three-dimensional structure of NC from the NCBI database (https://www.ncbi.nlm.nih.gov/pccompound/), it was uploaded to PharmMapper database [26] (http://www.lilab-ecust.cn/pharmmapper/) for further analysis. Utilizing the reverse pharmacophore matching method, the pharmacophore model of the drug was selected. Subsequently, the final 300 protein conformations were meticulously analyzed to obtain the target name, gene name, UniProt ID, and other relevant results pertaining to NC. Simultaneously, the Canonical SMILES of NC was uploaded to the SwissTargetPrediction database (http://www.swisstargetprediction.ch/). Behind, we imported the targets of NC obtained from the two databases into the UniProt database (https://www.Uniprot.org/), with selection of "*Homo sapiens*" as the appropriate species. To ensure the accuracy and reliability of our data, non-human targets and duplicated targets were subsequently removed. The resulting set of targets represented the relevant targets of NC for further analysis.

2.2. Acquisition of HCC targets

To ensure the specificity and relevance of the targets we obtained, we chose to obtain the corresponding targets from datasets in the GEO database that were previously confirmed to be specifically associated with HCC. This approach allowed us to focus specifically on the targets that were most relevant to our study of HCC, and ensured the validity of our subsequent analyses. We searched the GEO database to find relevant ChIP data using "hepatocellular carcinoma" as the search phrase. In the study, the following criteria were applied to select the appropriate datasets for analysis: (1) the species was limited to *Homo sapiens*; (2) the sample type was restricted to "tissue"; (3) the liver cancer type was HCC; (4) both normal (including normal or adjacent tissue) and tumor groups were included; (5) the sample size was greater than 30. The raw data were subjected to analysis using GEO2R to identify differentially expressed genes.

Specifically, HCC-related targets were identified by selecting genes with log2(foldchange) greater than 1 and *P*-value less than 0.05 in the normal and tumor groups.

2.3. Construction of protein-protein interaction network

The intersection of NC and HCC-related targets was utilized to identify potential targets for the treatment of HCC using NC. These potential targets were then inputted into the STRING database (http://string-db.org/), with the species limited to humans, to obtain a protein interaction network file for the identified targets. Cytoscape 3.8.2 was employed to visualize the protein-protein interaction (PPI) network.

2.4. Bioinformatics analysis of NC anti-HCC targets

The DAVID database(https://david.ncifcrf.gov/) was utilized for Gene Ontology (GO) and Kyoto Encyclopedia of Genes and Genomes (KEGG) enrichment analysis of NC anti-HCC targets. Upon downloading the analysis results, Microsoft Excel was employed for data cleaning, followed by the utilization of the ggplot2 package in the R software for visualization purposes. Furthermore, the relative mRNA expression levels of the target genes studied were analyzed online using the GEPIA website(http://gepia.cancer-pku.cn/).

2.5. In vitro experimental verification

2.5.1. Reagents

NC was purchased from Chengdu Herbpurify co.,LTD. Dulbecco's modified Eagle's medium(DMEM), RPMI 1640 and fetal bovine serum were purchased from Gibco (USA). Cell Counting Kit-8(CCK-8) was purchased from the MedChemExpress (USA). Cell Cycle and Apoptosis Analysis Kit and TRIzol reagent were purchased from Beyotime Biotechnology (China). TB Green® Fast qPCR Mix was purchased from TaKaRa (Japan). The PCR primers were purchased from Sangon Biotech Co., Ltd. (China). p53, 14-3-3 Sigma, CDK1 and GAPDH primary antibodies were purchased from Proteintech Group, Inc(China).

2.5.2. Cell viability assay

Hep G2 and LO2 cells were cultured in DMEM, while Huh 7 cells were cultured in RPMI 1640. The culture medium for all cell lines consisted of 10 % fetal bovine serum, 100 U/mL penicillin, and 0.1 mg/mL streptomycin. The cells were maintained at 37 °C with 5 % CO2. Each cell line was divided into four groups, and each group had five parallel replicates. Huh 7, Hep G2, and LO2 cells in the logarithmic growth phase were seeded into 96-well plates at a density of 0.8 × 104 cells/well (100 μL). After 24 h, the cells were exposed to media containing different concentrations of NC (0, 5, 10, or 20 μM). Following 24 h of continued cultivation, 10 μL of CCK-8 solution was added to each well, and the plates were incubated in the incubator for 2 h before testing.

2.5.3. Cell cycle phases assay

Huh 7 and Hep G2 cells were cultured in 6-well trays and treated with a solution containing 20 μM NC. After 24 h of treatment, the cells were harvested and washed with phosphate-buffered saline (PBS). Subsequently, the cells were fixed using a fixation solution (70 % ethanol). The rate of cell cycle phases (G1, S, and G2/M) was measured using a Cell Cycle and Apoptosis Analysis Kit, following the manufacturer's instructions. The stained cells were sorted, and data were acquired using a BD FACSCanto Plus flow cytometer (BD Biosciences, USA).

2.5.4. Real-time qPCR

Huh 7 and Hep G2 cells were treated with a solution containing 20 μM NC for 24 h. Total RNA was extracted from each group using the TRIzol reagent. Complementary DNA (cDNA) was synthesized using random hexamer primers and a SuperScript III reverse transcriptase kit. Following reverse transcription, a 20-μL aliquot was used for quantitative polymerase chain reaction (qPCR) to analyze the relative mRNA expression. The results were analyzed using the $2^{-\Delta\Delta Ct}$ method. The primer sequences are provided in **Table 1**.

2.5.5. Western blot

Huh 7 and Hep G2 cells were treated with a solution containing 20 μM NC for 24 h. Total protein was extracted from the Huh 7 and Hep G2 cells, respectively. The bicinchoninic acid (BCA) protein assay kit was used to analyze the concentrations of total protein, following the manufacturer's protocol. Protein from Huh 7 and Hep G2 cells was isolated using SDS-PAGE with a 10 % separating gel.

Table 1
Primer sequences.

Target Gene	Forward primer (5′- 3′)	Reverse primer (5′- 3′)
p53	TCTACAAGCAGTCACAGCACAT	CAACCTCAGGCGGCTCATAG
14-3-3 Sigma	CTGGACTCGCACCTCATCAA	GGCTGTTGGCTATCTCGTAGT
CDK1	CAGGTCAAGTGGTAGCCATGA	CAGGTCAAGTGGTAGCCATGA
Actin	TGGCACCCAGCACAATGAA	CTAAGTCATAGTCCGCCTAGAAGCA

After electrophoresis, the proteins were transferred onto a PVDF membrane. Subsequently, the primary antibodies p53, 14-3-3 Sigma, CDK1, and GAPDH were incubated overnight at 4 °C. The next day, the membranes were incubated for 1 h with the secondary antibody in a dark environment. Finally, the relative expressions of various proteins were quantified using Image-J. The grey densities of the protein bands were normalized using GAPDH density as an internal control.

2.5.6. Statistical analysis

SPSS 20.0 was utilized for statistical analysis, and differences between the groups were evaluated using a Student's t-test. The data are presented as mean ± SD, and comparisons with a p-value of less than 0.05 were considered statistically significant.

3. Results

3.1. Anti-HCC targets of NC

A total of 176 human NC targets were collected from the PharmMapper and SwissTargetPrediction databases. In order to fulfill the inclusion criteria for the ChIP analysis, four datasets (GSE135631, GSE105130, GSE124535, and GSE169289) were screened, and their gene expression differences were analyzed (Fig. 1A–D). The overlapping genes between normal tissue and tumor tissue in these chips were identified as HCC targets, resulting in a total of 1293 genes(Fig. 2A). Subsequently, the intersection of NC targets and HCC targets yielded a total of 24 NC anti-HCC targets (Fig. 2B).

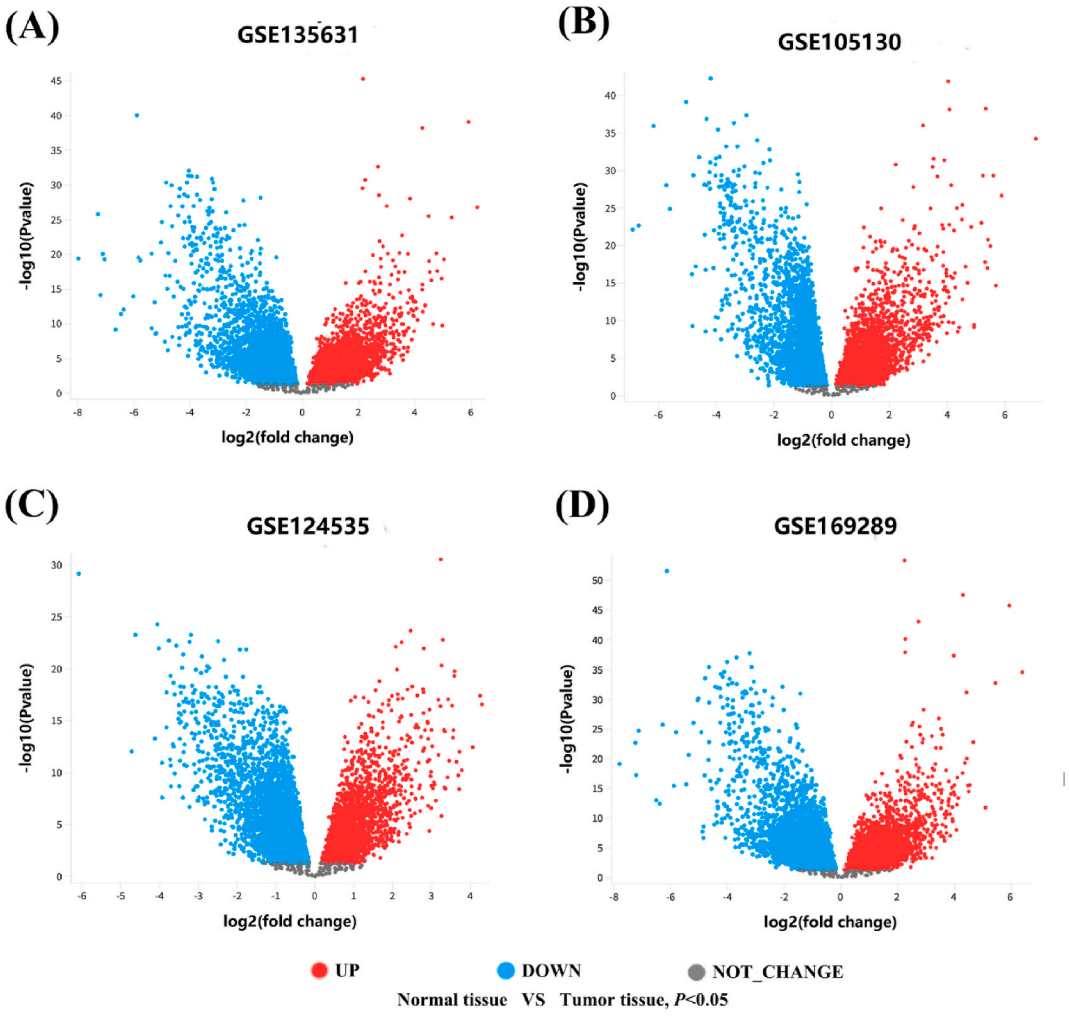

Fig. 1. Gene difference analysis of chip GSE135631, GSE105130, GSE124535, and GSE169289.

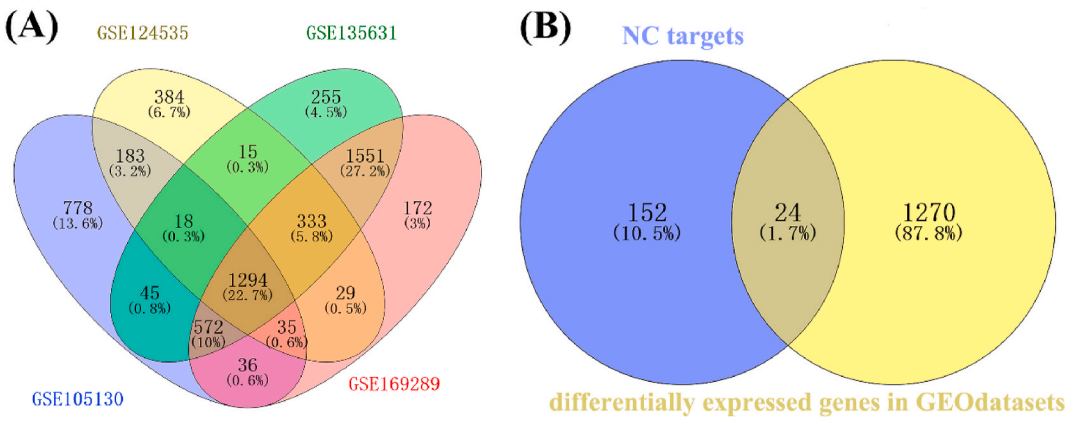

Fig. 2. Venn diagram for shared differentially expressed genes on the chips and NC anti-HCC targets. Notes: (A) Venn diagram for shared differentially expressed genes on the chips; (B) Venn diagram for NC anti-HCC targets.

3.2. PPI network

The STRING database was utilized to generate data for a network of 24 target-related PPI network (Fig. 3A). Subsequently, the interaction relationships of these 24 targets were imported into Cytoscape to construct a functional-related protein interaction network (Fig. 3B).

3.3. Biological function and pathway enrichment analyses

The anti-HCC targets of NC were subjected to GO and KEGG enrichment analyses using the David database. The results demonstrated that the 24 targets were associated with 38 biological processes (BP), 19 cell components (CC), and 20 molecular functions (MF). These processes encompassed a wide range of functions such as G2/M transition of the mitotic cell cycle, organic acid metabolic process, protein phosphorylation, spindle microtubule, centrosome, aromatase activity, heme binding, and protein serine/threonine kinase activity. To visualize the top 10 gene functions, a bar graph was generated using R 4.2.3 software (Fig. 4). Additionally, the KEGG pathway enrichment analysis unveiled the involvement of the 24 targets in regulating 10 signaling pathways, which were depicted in bubble maps using R 4.2.3 software (Fig. 5). These results suggested that the mechanism of NC treatment for HCC may be associated with the cell cycle (specifically the G2/M phase) and the p53 signaling pathway. Additionally, the relevant genes were labeled in Fig. 3B.

3.4. NC inhibits Huh 7 and Hep G2 cells proliferation and inducts of G2/M cell cycle arrest

In order to prove that NC can inhibit the proliferation of HCC cells and has no effect on normal hepatocytes, Huh 7, Hep G2 and LO2 cells were given NC solutions of different concentrations (0 μM, 5 μM, 10 μM, 20 μM). The results showed that NC had little inhibitory effect on LO2 cells, but had significant inhibitory effect on Huh 7 and Hep G2 cells (Fig. 6).

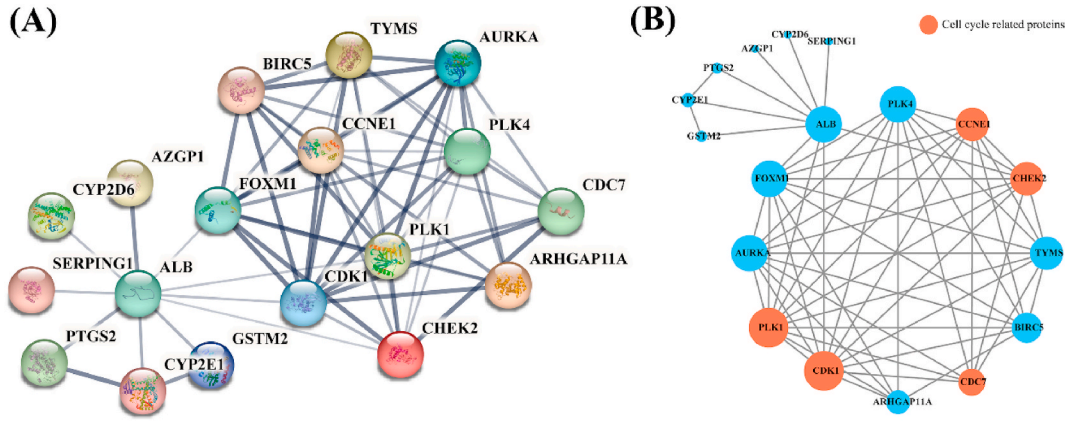

Fig. 3. Protein-protein interaction network of NC anti-HCC targets. Notes: (A) Target-related PPI network. (B) Functional-related protein interaction network.

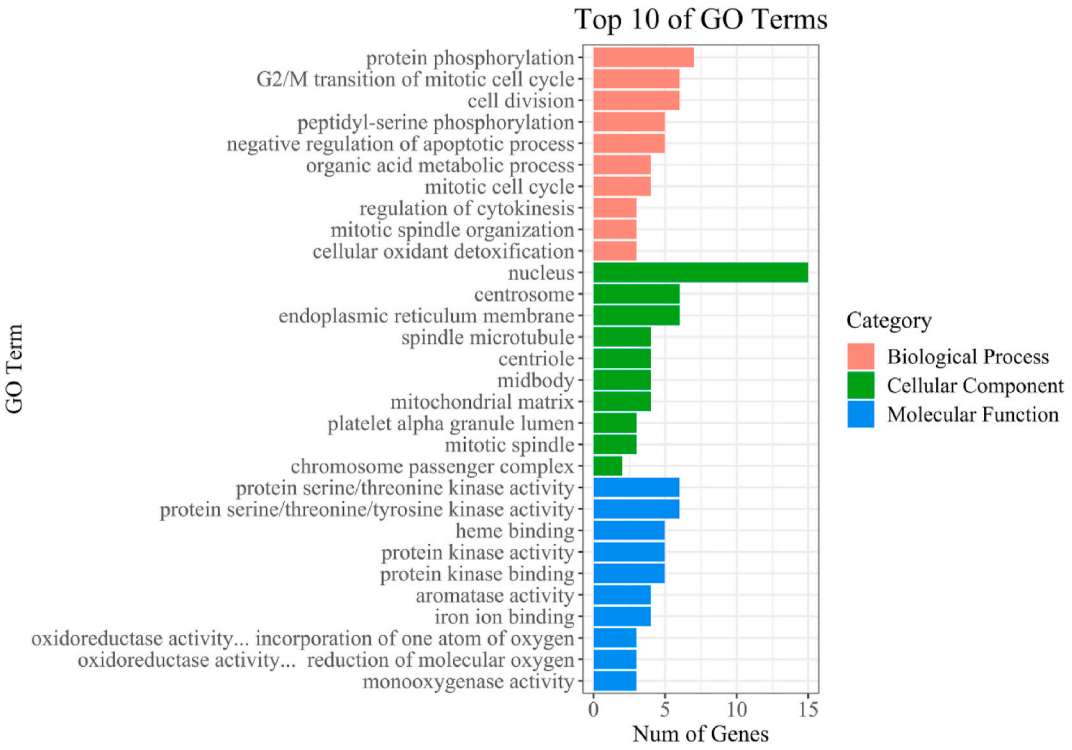

Fig. 4. GO enrichment analysis for 24 NC anti-HHC targets.

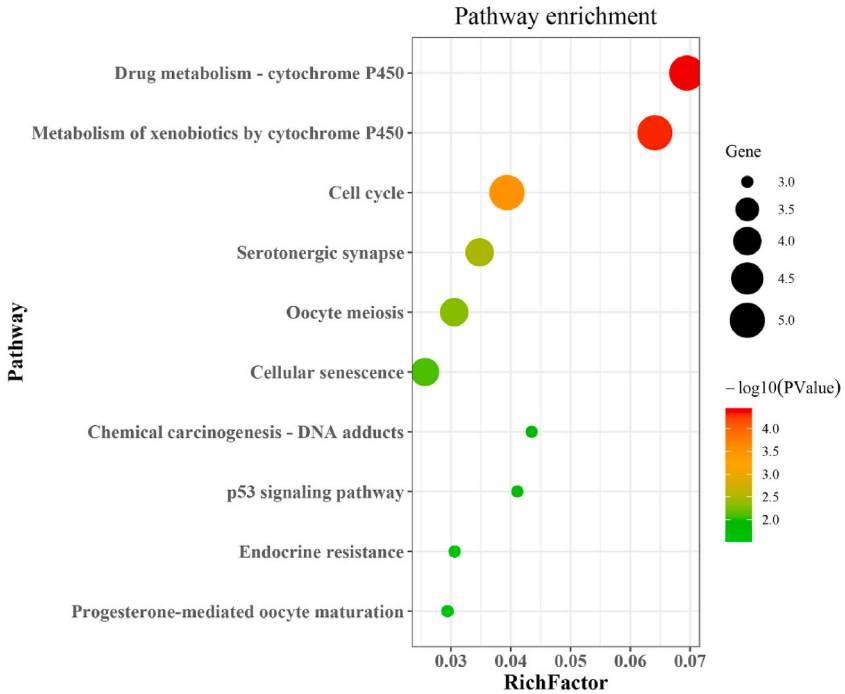

Fig. 5. KEGG pathway analysis for 24 NC anti-HHC targets.

To verify the predicted results of network pharmacology, we examined the cell cycle intervention of NC on HCC cells by flow cytometry. As shown in Fig. 7, G2/M-phase cell accumulation was observed in the NC-added Huh 7(Fig. 7A) and Hep G2 cells(Fig. 7B). It suggested that NC could exert its inhibitory effect on HCC cells by regulating G2/M-phase.

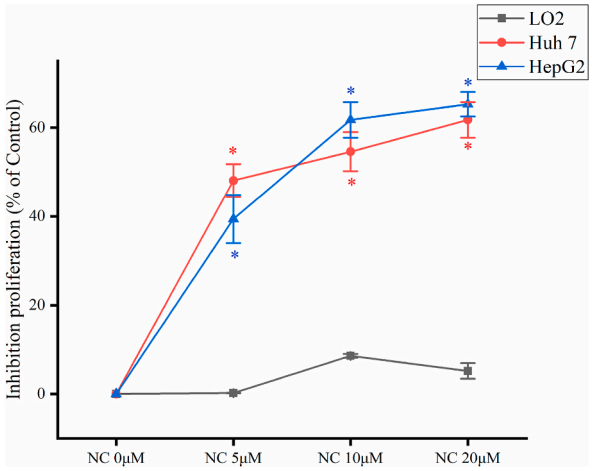

Fig. 6. Inhibition of Huh 7, Hep G2 and LO2 proliferation. Notes: The inhibition of Huh 7, Hep G2 and LO2 proliferation (% of Control). n = 3. Data are presented as means ± SD.

3.5. The mRNA and protein expression of p53, 14-3-3 Sigma and CDK1 in Huh 7 and Hep G2 cells

GO and KEGG enrichment analyses indicated that NC treatment of HCC was potentially related to the cell cycle and p53 signaling pathways. Furthermore, our in vitro experiments confirmed that NC increased the number of cells in the G2/M phase. Upon analyzing the p53 signaling pathway, it was observed that p53 regulated 14-3-3 Sigma and then interfered with CDK1, thereby impacting the G2/M phase of cells.

Therefore, we conducted an analysis of the relative expression of p53, 14-3-3 Sigma, and CDK1 mRNA in normal tissues and tumor tissues using the GEPIA website. The results showed that there was no significant difference in p53 mRNA expression in tumor tissues compared with normal tissues; Meanwhile, the relative expression levels of 14-3-3 Sigma and CDK1 mRNA were significantly higher in

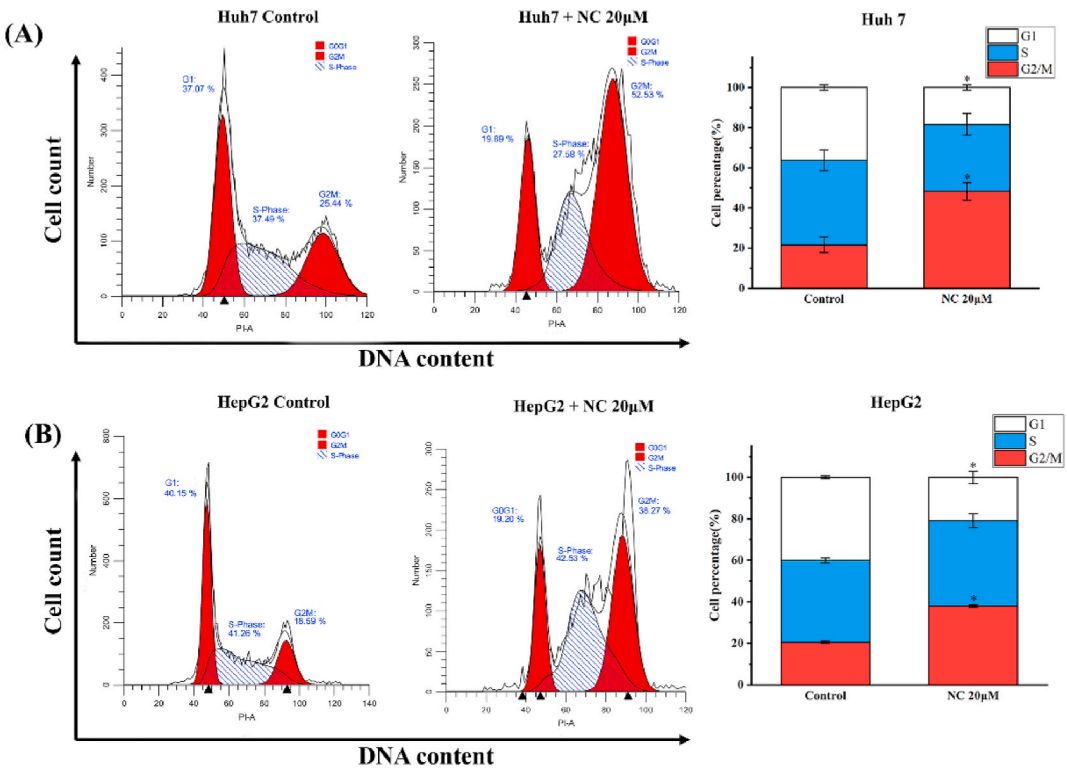

Fig. 7. NC induces cell cycle arrest of Huh 7 and Hep G2 cells. Notes: (A) NC induces cell cycle arrest of Huh 7 cells. (B) NC induces cell cycle arrest of Hep G2 cells. n = 3. Data are presented as means ± SD, $^*P < 0.05$.

tumor tissues compared to normal tissues (Fig. 8). In addition, our results showed that after NC treatment, the expression of p53 mRNA in Huh 7 and Hep G2 cells was significantly increased, while the expression of 14-3-3 Sigma and CDK1 mRNA was significantly decreased (Fig. 9A–F). Finally, Western blot results showed that NC significantly promoted the expression of p53 protein in Huh 7 and Hep G2 cells, while inhibited the expression of 14-3-3 Sigma and CDK1 proteins (Fig. 10A–C). These results suggest that NC may have a role in the treatment of HCC by modulating the p53/14-3-3 Sigma/CDK1 axis.

4. Discussion

This study investigates the mechanism of NC in treating HCC through network pharmacology and in vitro experimentation. Multiple database analyses identified 24 NC anti-HCC targets. Subsequent GO and KEGG enrichment analyses of these targets suggested that NC treatment of HCC may be associated with the cell cycle, specifically the G2/M phase, and the p53 signaling pathways. Our in vitro results provide additional support for these findings. Additionally, we discovered that the p53/14-3-3 Sigma/CDK1 axis within the p53 signaling pathway plays a crucial role in the effectiveness of NC treatment for HCC.

Cancer is invariably linked to abnormal regulation of the cell cycle process [27]. Numerous studies have reported that active ingredients found in traditional Chinese medicine can impede the proliferation of cancer cells by disrupting the cell cycle. Echinacoside, the principal active ingredient of *Cistanches* Herba, is known for its therapeutic effects on metastatic tumors. Li Wen et al. discovered that echinacoside inhibited the proliferation of Huh7 and HepG2 cells by arresting the cells in the S phase [28]. Pu Zhongjian et al. treated HepG2 cell lines with various concentrations of matrine, and the results suggested that matrine could inhibit HepG2 cell proliferation by arresting the cells in the G2/M phase [29]. Curcumin, a yellow pigment extracted from the rhizome of turmeric, exhibits a wide range of pharmacological activities [30]. Bai Chunhua et al. observed that curcumin, at different concentrations, could arrest HepG2 and SK-Hep-1 cells in the G0/G1 phase [31]. Signaling pathways monitor the successful completion of preceding events before progressing to the subsequent phase at crucial transitions during eukaryotic cell cycle progression. These regulatory pathways are commonly referred to as cell cycle checkpoints [32]. In cancer, these cell checkpoints are often deactivated due to genetic mutations [31]. Our network pharmacological results suggest that the mechanism underlying the treatment of HCC with NC may be associated with the cell cycle, particularly the G2/M phase. Therefore, we employed flow cytometry to detect changes in the cell cycle of Huh7 and G2 cell lines following NC treatment. The results demonstrated that NC could arrest HCC cells in the G2/M phase. In addition, KEGG analysis indicated that NC treatment of HCC may be related to p53 signaling pathway.

The p53 signaling pathway represents a complex network within the cell that responds to various stress signals and contributes to its role as a tumor suppressor pathway [33]. Numerous studies have demonstrated the involvement of p53 in crucial biological processes such as cell cycle arrest and apoptosis in HCC [34,35]. CDKN1A, which encodes the p21 protein, is a major inducer of p53-mediated cell cycle arrest [36]. It has been observed that p21 interacts with cyclin E/CDK2 and cyclin D/CDK4, facilitating the binding of Rb to E2F, consequently leading to G1 arrest [37]. Moreover, p53 exerts control over the cell cycle by regulating the transcription of 14-3-3 Sigma, resulting in G2/M arrest [38]. Mechanistically, this process involves the inhibition of the cyclin B and CDK1 complex by 14-3-3 Sigma, ultimately causing G2/M phase arrest [38]. Interestingly, our analysis of the TCGA database revealed elevated expressions of 14-3-3 Sigma, and CDK1 genes in cancer tissues compared to normal tissues. Notably, CDK1 is also one of the targets for NC therapy in HCC.

The 14-3-3 Sigma protein, initially identified as a cell cycle inhibitor regulated by p53, responds to DNA damage caused by γ irradiation and other DNA-damaging agents. Its activation is facilitated by a p53-responsive element located 1.8 kb upstream of its transcription start site [39]. The 14-3-3 family members possess the ability to interact with more than 100 functionally diverse cellular proteins, playing critical roles in various cellular processes such as signal transduction, cell cycle regulation, apoptosis, cytoskeletal organization, and malignant transformation [40]. The 14-3-3 family members possess the ability to interact with more than 100 functionally diverse cellular proteins, playing critical roles in various cellular processes such as signal transduction, cell cycle regulation, apoptosis, cytoskeletal organization, and malignant transformation [41]. Dysregulation of CDK1 activity disrupts precise genetic material delivery, thereby affecting normal cell cycle function [42]. As the loss of cell cycle control is a key factor in tumor growth [43], maintaining proper CDK1 expression is crucial.

In our study, in vitro experiments showed that NC treatment resulted in increased p53 mRNA and protein expression and decreased 14-3-3 Sigma and CDK1 mRNA and protein expression in Huh 7 and G2 cell lines. These findings suggest that the anti-HCC effect of NC may be mediated through the regulation of the p53/14-3-3 Sigma/CDK1 axis, inducing G2/M arrest in HCC cells. Compared with previous studies on the treatment of HCC with NC, we further elucidated the possible mechanism of NC blocking cell cycle, and further expanded the target of NC anti-HCC. Therefore, our study contributes to the development of NC as a prototype drug or precursor drug against HCC, and provides further theoretical basis for its clinical development.

5. Conclusion

In summary, NC can inhibit the proliferation of HCC cells and induce G2/M cell cycle arrest, potentially by regulating the p53/14-3-3 Sigma/CDK1 axis.

Funding

Our study was supported by Guangxi natural science foundation (No. 2022GXNSFDA 035063, No. 2023GXNSFAA026366) and Innovation Project of Guangxi College Students Education (S202310601111).

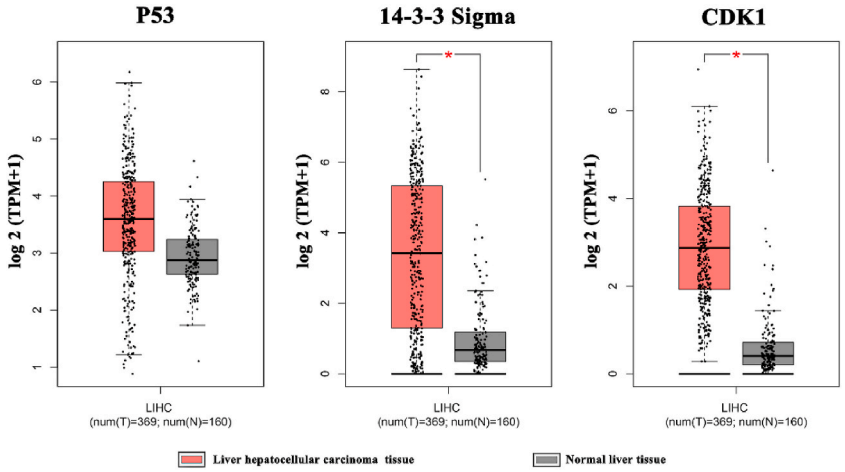

Fig. 8. The mRNA expression of p53, 14-3-3 Sigma and CDK1 in HCC from TCGA data.

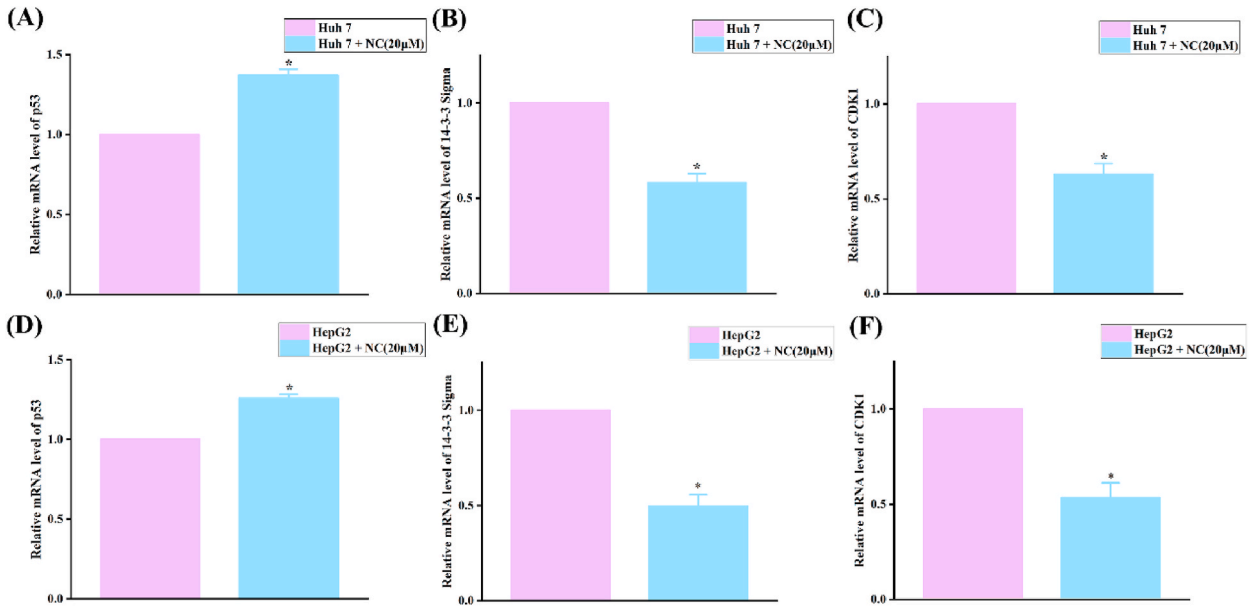

Fig. 9. The mRNA expression of p53, 14-3-3 Sigma and CDK1 in Huh 7 and Hep G2 cells. Notes: (A) The expression levels of p53 mRNA in Huh 7 cells; (B) The expression levels of 14-3-3 Sigma mRNA in Huh 7 cells; (C) The expression levels of CDK1 mRNA in Huh 7 cells; (D) The expression levels of p53 mRNA in Hep G2 cells; (E) The expression levels of 14-3-3 Sigma mRNA in Hep G2 cells; (F) The expression levels of CDK1 mRNA in Hep G2 cells. n = 3. Data are presented as means ± SD. *$P < 0.05$, compared with Huh 7(Hep G2) group.

Data availability statement

The data associated with our study has been deposited into a publicly available repository. These data can be found here: GEO: GSE135631, GSE105130, GSE124535, and GSE169289. WB raw data has been submitted as supplementary material. The other data used to support the findings of this study are included in the article.

CRediT authorship contribution statement

Bo Zhang: Writing - original draft. **Bo Zhou:** Methodology, Formal analysis. **Guihong Huang:** Visualization, Software. **Jing'an Huang:** Validation. **Xiaoxin Lin:** Validation. **Zonghuai Li:** Validation. **Yuanchu Lian:** Validation. **Qiujie Huang:** Writing - review & editing. **Yong Ye:** Writing - review & editing, Resources.

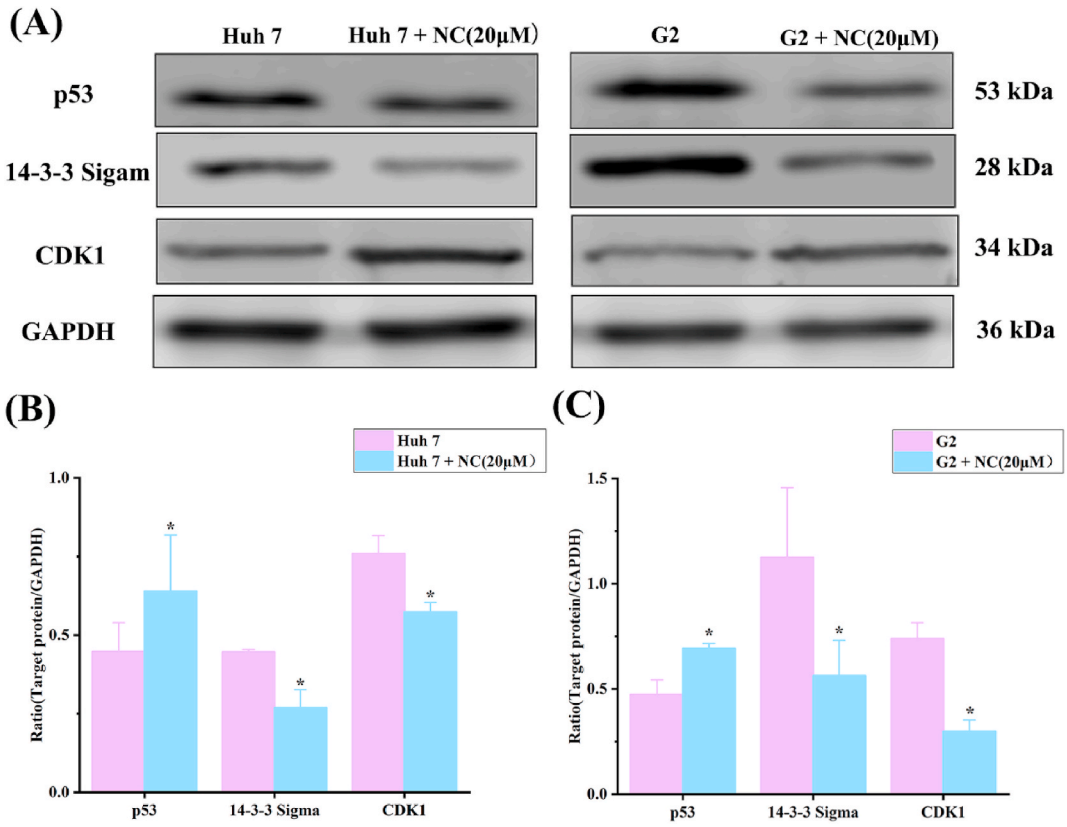

Fig. 10. The protein expression of p53, 14-3-3 Sigma and CDK1 in Huh 7 and Hep G2 cells. Full, non-adjusted blot images are provided in Supplementary Materials S1. Notes: (A) Western blot analysis of p53, 14-3-3 Sigma and CDK1 in Huh 7 and Hep G2 cells. (B) The expression levels of p53, 14-3-3 Sigma and CDK1 protein in Huh 7 cells; (C) The expression levels of p53, 14-3-3 Sigma and CDK1 protein in Hep G2 cells; *$P < 0.05$, compared with Huh 7(Hep G2) group.

Declaration of competing interest

The authors declare that they have no known competing financial interests or personal relationships that could have appeared to influence the work reported in this paper.

Appendix A. Supplementary data

Supplementary data to this article can be found online at https://doi.org/10.1016/j.heliyon.2024.e24012.

Abbreviations

BP	biological processes
CC	cell components
GO	Gene Ontology
HCC	hepatocellular carcinoma
KEGG	Kyoto Encyclopedia of Genes and Genomes
MF	molecular functions
NC	Nitidine chloride
PPI	protein-protein interaction
qPCR	quantitative polymerase chain reaction

References

[1] H. Sung, J. Ferlay, R.L. Siegel, et al., Global cancer Statistics 2020: GLOBOCAN estimates of incidence and mortality worldwide for 36 cancers in 185 countries, CA A Cancer J. Clin. 71 (3) (2021) 209–249.
[2] W.S. Yang, X.F. Zeng, Z.N. Liu, et al., Diet and liver cancer risk: a narrative review of epidemiological evidence, Br. J. Nutr. 124 (3) (2020) 330–340.
[3] M. Ringelhan, J.A. McKeating, U. Protzer, Viral hepatitis and liver cancer, Philos. Trans. R. Soc. Lond. Ser. B Biol. Sci. (1732) (2017) 372.
[4] C.H. Chiang, C.S. Kuo, W.W. Lin, et al., Chronic viral hepatitis signifies the association of premixed insulin analogues with liver cancer risks: a nationwide population-based study, Int. J. Environ. Res. Publ. Health 16 (12) (2019).
[5] C. Shen, X. Jiang, M. Li, et al., Hepatitis virus and hepatocellular carcinoma: recent advances, Cancers 15 (2) (2023).
[6] F. Wu, J.D. Groopman, J.J. Pestka, Public health impacts of foodborne mycotoxins, Annu. Rev. Food Sci. Technol. 5 (2014) 351–372.
[7] J.D. Groopman, J.W. Smith, A. Rivera-Andrade, et al., Aflatoxin and the etiology of liver cancer and its implications for Guatemala, World Mycotoxin J. 14 (3) (2021) 305–317.
[8] M. Karin, D. Dhar, Liver carcinogenesis: from naughty chemicals to soothing fat and the surprising role of NRF2, Carcinogenesis 37 (6) (2016) 541–546.
[9] P. Shah, P. Shende, Biomacromolecule-functionalized nanoparticle-based conjugates for potentiation of anticancer therapy, Curr. Cancer Drug Targets 22 (1) (2022) 31–48.
[10] Y. Zhang, Y. Qu, Y.Z. Chen, Influence of 6-shogaol potentiated on 5-fluorouracil treatment of liver cancer by promoting apoptosis and cell cycle arrest by regulating AKT/mTOR/MRP1 signalling, Chin. J. Nat. Med. 20 (5) (2022) 352–363.
[11] Y. Kawano, M. Tanaka, M. Fujishima, et al., Acanthopanax senticosus Harms extract causes G0/G1 cell cycle arrest and autophagy via inhibition of Rubicon in human liver cancer cells, Oncol. Rep. 45 (3) (2021) 1193–1201.
[12] A. Abusaliya, S.H. Jeong, P.B. Bhosale, et al., Mechanistic action of cell cycle arrest and intrinsic apoptosis via inhibiting Akt/mTOR and activation of p38-MAPK signaling pathways in Hep3B liver cancer cells by Prunetrin-A flavonoid with therapeutic potential, Nutrients 15 (15) (2023).
[13] Q. Lu, R. Ma, Y. Yang, et al., Zanthoxylum nitidum (Roxb.) DC: traditional uses, phytochemistry, pharmacological activities and toxicology, J. Ethnopharmacol. 260 (2020) 112946.
[14] H. Liu, J. Feng, K. Feng, et al., Optimization of the extraction conditions and quantification by RP-LC analysis of three alkaloids in Zanthoxylum nitidum roots, Pharmaceut. Biol. 52 (2) (2014) 255–261.
[15] F. Qin, C.Y. Wang, C.G. Wang, et al., Undescribed isoquinolines from Zanthoxylum nitidum and their antiproliferative effects against human cancer cell lines, Phytochemistry 205 (2023) 113476.
[16] C.Y. Wang, F. Qin, C.G. Wang, et al., Novel lignans from Zanthoxylum nitidum and antiproliferation activity of sesaminone in osimertinib-resistant non-small cell lung cancer cells, Bioorg. Chem. 134 (2023) 106445.
[17] H. Mou, P. Guo, X. Li, et al., Nitidine chloride inhibited the expression of S phase kinase-associated protein 2 in ovarian cancer cells, Cell Cycle 16 (14) (2017) 1366–1375.
[18] L.M. Liu, D.D. Xiong, P. Lin, et al., DNA topoisomerase 1 and 2A function as oncogenes in liver cancer and may be direct targets of nitidine chloride, Int. J. Oncol. 53 (5) (2018) 1897–1912.
[19] H. Xu, T. Cao, X. Zhang, et al., Nitidine chloride inhibits SIN1 expression in osteosarcoma cells, Molecular Therapy Oncolytics 12 (2019) 224–234.
[20] M. Liu, J. Wang, Q. Qi, et al., Nitidine chloride inhibits the malignant behavior of human glioblastoma cells by targeting the PI3K/AKT/mTOR signaling pathway, Oncol. Rep. 36 (4) (2016) 2160–2168.
[21] J. Chen, J. Wang, L. Lin, et al., Inhibition of STAT3 signaling pathway by nitidine chloride suppressed the angiogenesis and growth of human gastric cancer, Mol. Cancer Therapeut. 11 (2) (2012) 277–287.
[22] J. Liao, T. Xu, J.X. Zheng, et al., Nitidine chloride inhibits hepatocellular carcinoma cell growth in vivo through the suppression of the JAK1/STAT3 signaling pathway, Int. J. Mol. Med. 32 (1) (2013) 79–84.
[23] S. Chen, Y. Liao, J. Lv, et al., Quantitative proteomics based on iTRAQ reveal that nitidine chloride induces apoptosis by activating JNK/c-Jun signaling in hepatocellular carcinoma cells, Planta Med. 88 (13) (2022) 1233–1244.
[24] J. Lin, A. Shen, H. Chen, et al., Nitidine chloride inhibits hepatic cancer growth via modulation of multiple signaling pathways, BMC Cancer 14 (2014) 729.
[25] X. Ou, Y. Lu, L. Liao, et al., Nitidine chloride induces apoptosis in human hepatocellular carcinoma cells through a pathway involving p53, p21, Bax and Bcl-2, Oncol. Rep. 33 (3) (2015) 1264–1274.
[26] X. Liu, S. Ouyang, B. Yu, et al., PharmMapper server: a web server for potential drug target identification using pharmacophore mapping approach, Nucleic Acids Res. 38 (2010) W609–W614. Web Server issue).
[27] J. Li, H.Y. Huang, Y.C. Lin, et al., Cinnamomi ramulus inhibits cancer cells growth by inducing G2/M arrest, Front. Pharmacol. 14 (2023) 1121799.
[28] W. Li, J. Zhou, Y. Zhang, et al., Echinacoside exerts anti-tumor activity via the miR-503-3p/TGF-β1/Smad aixs in liver cancer, Cancer Cell Int. 21 (1) (2021) 304.
[29] Z.J. Pu, Y.J. Wang, F. Ge, et al., Matrine induces cell cycle arrest and apoptosis in hepatocellular carcinoma cells via miR-122 mediated CG1/livin/survivin signal axis, Trop. J. Pharmaceut. Res. 20 (2) (2021) 263–268.
[30] S.C. Gupta, B. Sung, J.H. Kim, et al., Multitargeting by turmeric, the golden spice: from kitchen to clinic, Mol. Nutr. Food Res. 57 (9) (2013) 1510–1528.
[31] C.H. Bai, J.Q. Zhao, J.L. Su, et al., Curcumin induces mitochondrial apoptosis in human hepatoma cells through BCLAF1-mediated modulation of PI3K/AKT/GSK-3? signaling, Life Sci. 306 (2022) 10.
[32] L.H. Hartwell, T.A. Weinert, Checkpoints: controls that ensure the order of cell cycle events, Science (New York, NY) 246 (4930) (1989) 629–634.
[33] L.J. Hernández Borrero, W.S. El-Deiry, Tumor suppressor p53: biology, signaling pathways, and therapeutic targeting, Biochim. Biophys. Acta, Rev. Cancer 1876 (1) (2021) 188556.
[34] S. Rebouissou, J.C. Nault, Advances in molecular classification and precision oncology in hepatocellular carcinoma, J. Hepatol. 72 (2) (2020) 215–229.
[35] J. Krstic, M. Galhuber, T.J. Schulz, et al., p53 as a dichotomous regulator of liver disease: the dose makes the medicine, Int. J. Mol. Sci. 19 (3) (2018).
[36] W.S. el-Deiry, T. Tokino, V.E. Velculescu, et al., WAF1, a potential mediator of p53 tumor suppression, Cell 75 (4) (1993) 817–825.
[37] Z.A. Stewart, S.D. Leach, J.A. Pietenpol, p21(Waf1/Cip1) inhibition of cyclin E/Cdk2 activity prevents endoreduplication after mitotic spindle disruption, Mol. Cell Biol. 19 (1) (1999) 205–215.
[38] H. Hermeking, C. Lengauer, K. Polyak, et al., 14-3-3sigma is a p53-regulated inhibitor of G2/M progression, Mol. Cell 1 (1) (1997) 3–11.
[39] A. Shiba-Ishii, Significance of stratifin in early progression of lung adenocarcinoma and its potential therapeutic relevance, Pathol. Int. 71 (10) (2021) 655–665.
[40] H. Hermeking, The 14-3-3 cancer connection, Nat. Rev. Cancer 3 (12) (2003) 931–943.
[41] J.M. Enserink, R.D. Kolodner, An overview of Cdk1-controlled targets and processes, Cell Div. 5 (2010) 11.
[42] P. Nurse, Cyclin dependent kinases and cell cycle control (nobel lecture), Chembiochem : a European journal of chemical biology 3 (7) (2002) 596–603.
[43] H.K. Matthews, C. Bertoli, R.A.M. de Bruin, Cell cycle control in cancer, Nat. Rev. Mol. Cell Biol. 23 (1) (2022) 74–88.